Technical Assessment of Solar Assisted Refrigeration Using Parabolic Trough Collectors in a Mexican Pharmaceutical Facility

Eduardo González-Mora[1], Ma. Dolores Durán-García[1]

[1] Ingeniería en Sistemas Energéticos Sustentables, Facultad de Ingeniería, Universidad Autónoma del Estado de México, Toluca (México)

Abstract

Industrial refrigeration underpins critical processes in the pharmaceutical sector and contributes significantly to energy consumption and emissions. Solar thermal cooling emerges as a promising alternative by harnessing concentrated solar irradiation to drive absorption chillers without fossil fuels. Absorption systems in pharmaceutical facilities typically rely on liquefied petroleum gas (LPG) to achieve low-temperature demands (-10 °C), resulting in high operational costs and carbon footprints. Here we address the feasibility of integrating medium-temperature parabolic trough collectors (PTCs) with and without thermal energy storage (TES) to meet a 118.2 kW cooling load in a Toluca, México, pharmaceutical plant. We applied a validated thermohydraulic model to size a 900 m² PTC array (no TES) and a 1350 m² array with 28.16 m³ TES, simulating design-day and annual performance under realistic irradiance and load profiles. Here we show that the PTC–TES configuration achieves daily LPG savings up to 500 kg (≈USD 300), attains solar coefficients of performance of 0.2407 (no TES) and 0.2219 (with TES), and increases the annual solar fraction from 40.7 % to 61.0 %. These results exceed prior solar cooling applications in food and mining by demonstrating rooftop PTC viability under area constraints and quantifying exergy benefits in a pharmaceutical context. Our findings advance the integration of renewable heat in industrial cooling, offering a replicable framework to decarbonize energy-intensive processes and support global climate targets.

Keywords: Solar cooling, parabolic trough collectors, thermal energy storage, industrial absorption refrigeration

1. Introduction

Industrial refrigeration is a cornerstone of global energy management and is essential for sustaining critical industrial processes, particularly in the energy and pharmaceutical sectors. In the energy domain, these systems account for approximately 17% of global electricity consumption, driving urgent efforts to enhance efficiency and transition to low-impact refrigerants, such as natural options like ammonia, CO_2, and advanced blends, to curb greenhouse gas emissions. (Mahmood, 2020). Innovations like waste heat recovery further amplify sustainability by repurposing excess thermal energy for district heating networks, reducing CO_2 footprints while improving energy integration. However, barriers such as high upfront costs and fragmented policy frameworks continue to impede the adoption of advanced technologies and low-GWP refrigerants, underscoring the need for coordinated action (IEA, 2018; Karellas et al., 2018). The REN21 report (2024) emphasizes that governments must prioritize renewable energy adoption across sectors and phase out fossil fuel dependencies, a stance that aligns with addressing these systemic challenges through policy incentives and infrastructure investments.

Concurrently, the pharmaceutical sector relies on industrial refrigeration for precise temperature control in drug manufacturing, storage, and vaccine production, demanding fail-safe systems that comply with stringent regulatory standards while balancing energy efficiency (Cabrera et al., 2013; Ouali et al., 2014; Permana and Wang, 2024). This dual focus on reliability and sustainability highlights the growing demand for innovative solutions that minimize downtime and environmental harm. Looking ahead, systemic shifts toward natural refrigerants, hybrid energy systems, and renewables-driven technologies are critical to reconciling operational efficiency with climate objectives, ensuring industrial refrigeration evolves as a catalyst for both sector-specific resilience and global decarbonization. By prioritizing sustainable alternatives, industries can align with

10.18086/swc.2025.02.25 Available at http://proceedings.ises.org

global decarbonization goals while building resilience against energy price fluctuations and regulatory pressures, ensuring long-term viability in a rapidly transitioning energy landscape.

Solar cooling technologies (SCT) leverage solar energy, primarily via thermal collectors like parabolic troughs (PTCs), to power refrigeration and air conditioning, cutting CO_2 emissions and electricity use. These systems are particularly viable for industrial cooling in sectors such as food processing, beverage, and mining, where demand aligns with solar availability. Key methods include absorption, adsorption, ejector, and desiccant cycles, driven by solar heat or photovoltaic electricity. PTCs concentrate sunlight to generate medium-high temperatures ideal for absorption cycles, while hybrid setups combining solar with conventional or PV-powered chillers ensure reliability during low sunlight (Cabrera et al., 2013; Karellas et al., 2018). Thermal energy storage (TES) further stabilizes these systems by storing excess heat for use during cloudy periods or nighttime, reducing backup energy reliance (Cabeza, 2014).

Solar-driven cooling systems offer an eco-friendly solution by harnessing freely available solar energy while eliminating pollution emissions. Recent advances in solar collectors, particularly in sorption refrigeration technologies, have enhanced system efficiency, as these collectors reliably deliver the precise operating temperatures critical for cooling performance. Their application is growing in industries like food processing and mining, where cooling demands align with solar availability (Cabrera et al., 2013; Esfanjani et al., 2022; Karellas et al., 2018). However, research gaps remain, particularly in adapting these systems for pharmaceutical applications in regions like Mexico, where studies are scarce. Further innovation in thermal storage and hybrid configurations could expand their viability, bridging technical and sector-specific challenges.

This study evaluates the technical performance and liquefied petroleum gas (LPG) savings potential of a parabolic trough collector (PTC)-driven absorption cooling system at a pharmaceutical facility in Toluca, México. The objectives include analyzing two system configurations—with and without thermal energy storage (TES)—under both design-day and annual operating conditions, with defined boundaries of a 2200 m² installation area and a -10°C cooling load. By coupling a solar thermal field to an existing LPG-fueled absorption chiller, the research quantifies energy savings and operational efficiency gains achievable through solar integration. The scope focuses on transitioning the facility's thermal energy supply from fossil fuel combustion to solar-driven processes, addressing gaps in region-specific applications of solar cooling technologies, particularly in México's pharmaceutical sector. Results aim to inform scalable strategies for reducing industrial carbon footprints while maintaining reliable cooling performance.

2. System description and case study

2.1. Pharmaceutical facility and cooling demand

The pharmaceutical facility under study, located in Toluca, México—a region with a dense industrial footprint—relies on a two-stage double-effect ammonia/water absorption refrigeration system with separate rectifiers to meet its low-temperature cooling demands. The system requires a net heat input of 292.2 kW, derived from LPG combustion, to generate a cooling output of 118.2 kW at -10°C, achieving a baseline coefficient of performance (β) of 0.405. With an available installation area of 2500 m^2, the facility aims to integrate a PTC solar field to replace a fossil fuel-based heat supply. Fig. 1 illustrates the schematic configuration of the absorption refrigeration system and the proposed PTC solar field integration, highlighting the coupling of solar heat to sustain the −10°C cooling load.

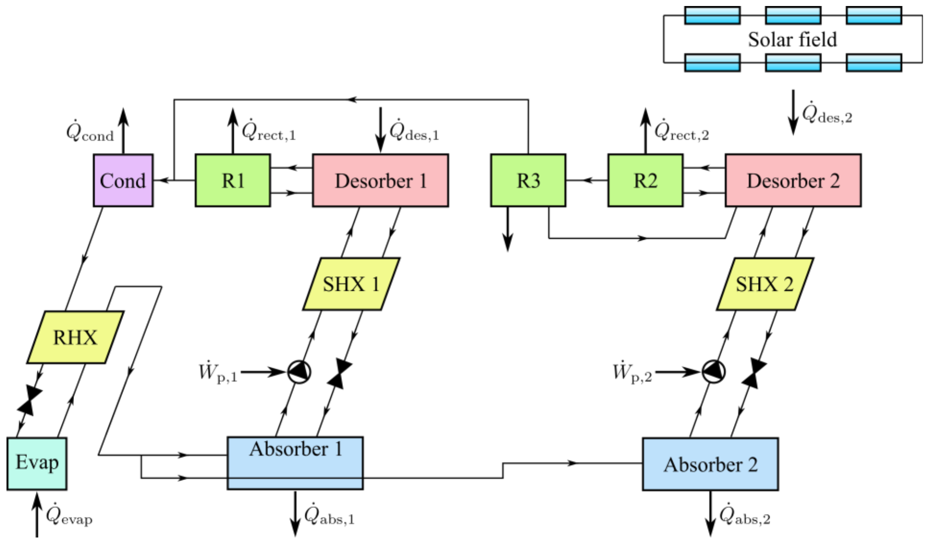

Fig. 1: Absorption refrigerator with solar field schematic.

2.2. Absorption refrigeration system description

The absorption refrigeration system in use is a commercially available two-stage double-effect ammonia/water system with separate rectifiers, currently operational in Mexico. This system relies on an ammonia/water mixture to achieve its cooling output of 118.2 kW at −10°C, operating with β=0.405 and $\eta_{II,ref}$ = 0.1705 (coefficient of performance and exergy efficiency). To sustain this performance, the facility burns 32.62 kg/h of LPG, incurring a daily fuel cost of approximately 782.9 USD. The refrigeration cycle's design—featuring dual stages and independent rectifiers—optimizes heat utilization while meeting stringent low-temperature industrial cooling demands. Key operational parameters and technical specifications of the system are summarized in Table 1, providing a detailed overview of its performance metrics and energy consumption profile.

Tab. 1: Summary data for the absorption refrigeration system

Parameter	Low temperature stage	High temperature stage
Vapor out of rectifier, (kg/s)	0.08081	0.02832
Desorber heat, (kW)	285.3	292.2
Vapor generation per unit of heat input, (kg/kJ)	2.83E-04	9.70E-05
Mass fraction of vapor out of desorber	0.9542	0.3097
Mass fraction of rich solution	0.3865	0.06081
Mass flow rate of rich solution, (kg/s)	1.3	0.6861
Liquid reflux, (kg/s)	8.06×10-02	5.09×10-03
Rectifier heat, (kW)	15.5	157
Absorber heat, (kW)	256.2	128.3
Solution heat exchanger heat, (kW)	254.9	151.9
Pump efficiency	0.77	0.77
High pressure, (bar)	15.4	15.4
Low pressure, (bar)	2.699	2.699
High temperature, (ºC)	112.2	191.4

Low temperature, (ºC)	84.3	163.4

2.3. Parabolic trough collector specification and TES system

The PTC represents the most mature and widely deployed concentrating solar technology, particularly suited for applications such as solar heat for industrial processes (SHIP). In industrial settings, small-scale PTC systems are commonly employed due to their adaptability and efficiency (Moya, 2021). For the present application, which requires heat delivery between 180°C and 200°C, the PTC is an optimal choice, as its operational range aligns precisely with these thermal demands. The proposed solar field will utilize compact PTC units, specifically the *Power Trough 250* model by Inventive Power, selected for its proven performance and local availability in México (Inventive Power, 2013). The facility's rooftop, with 2500 m^2 of available space, provides adequate area for installation.

Heat transfer fluid (HTF) selection is critical for system performance. Therminol VP1, the industry-standard HTF for PTCs, is chosen here due to its operational range of 100–400°C, which comfortably accommodates the required temperature elevation from 185°C to 210°C to meet the refrigeration process's heat demand. The system is analyzed under two configurations: one without thermal energy storage (TES) and another incorporating TES to enhance reliability (see Fig. 2). For the latter, a backup capacity of 2.5 hours and a solar multiple of 1.5 are specified to mitigate solar intermittency.

The TES system employs the same HTF (Therminol VP1) as the solar field, avoiding compatibility issues. A centralized single-tank thermocline design is proposed, leveraging thermal stratification to maintain distinct high- and low-temperature regions within the tank. This configuration eliminates the need for filler materials, simplifying construction and maintenance. However, detailed engineering of the TES tank, including stratification dynamics and sizing, falls outside the scope of this study.

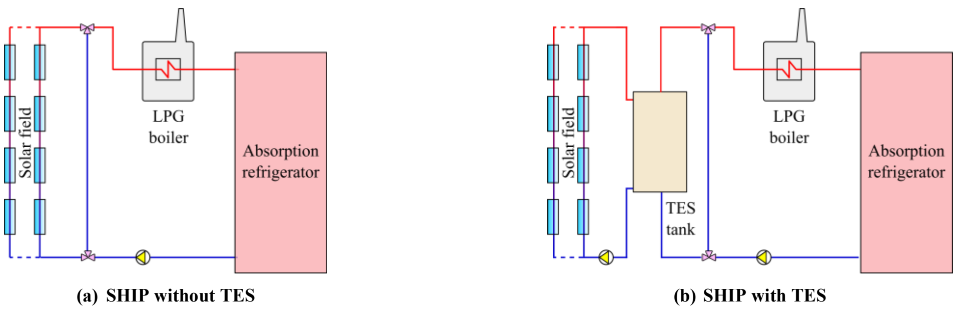

Fig. 2: Schematic diagrams of the SHIP installation.

The integration of these components forms a robust PTC-SHIP system, with technical operating specifications summarized in Table 2. This approach prioritizes operational feasibility, leveraging established technologies and locally available solutions to meet the industrial facility's thermal requirements efficiently.

Tab. 2: Specifications for the SHIP installation (Inventive Power, 2013)

Parameter	Symbol	Value
Parabolic trough collector		
Width, (m)	W	2.5
Focal length, (m)	f	0.930
Aperture area, (m2)	A_{ap}	10
Receiver outer/inner diameter, (m)	$d_{\mathrm{out}}/d_{\mathrm{in}}$	0.040/0.037
Glass cover outer/inner diameter, (m)	$d_{\mathrm{c,out}}/d_{\mathrm{c,in}}$	0.0572/0.0542
Peak optical efficiency	η_{o}	0.7355

Thermal energy storage		
Solar multiple	SM	1.5
Storage time, (h)	t_{storage}	2.5
Capacity, (kWh)	Q_{TES}	365.3
Refrigeration process conditions		
Process heat requirement, (kW)	$\dot{Q}_{\text{load}}$	292.2

3. Methodology

3.1. Thermal modelling framework

We employ the one-dimensional thermohydraulic model developed by González-Mora and Durán-García (2024). The model discretizes the receiver into smaller segments known as Heat Collector Elements (HCE) and includes comprehensive equations accounting for various parameters such as beam solar irradiation, optical and thermal losses, and the heat gains of the HTF as it flows through the solar field. Considering the solar energy redirected to the receiver, and the thermal losses, we establish an energy balance for the PTC receiver as follows:

$$\frac{\mathrm{d}E_{\text{PTC}}}{\mathrm{d}t} = \dot{Q}_{\text{in}} - \dot{Q}_{\text{loss}} = \dot{Q}_{\text{gain,HTF}} \qquad \text{(eq. 1)}$$

where $\mathrm{d}E_{\text{PTC}}/\mathrm{d}t$ represents the temporal change in the PTC's internal energy. The incoming solar power, $\dot{Q}_{\text{in}} = \eta_{\text{o}} W G_{\text{bn}}$, corresponds to the absorbed solar radiation influenced by the optical efficiency (η_{o}), the PTC's aperture (W) and the beam solar radiation (G_{bn}), while the heat losses, $\dot{Q}_{\text{loss}}$, include radiative, convective, and conductive losses. $\dot{Q}_{\text{gain,HTF}}$ is the net heat gain by the HTF. Following the procedure described by González-Mora and Durán-García (2024), we tailored the *Power Trough 250* PTC characteristics detailed in Table 1 to express the heat losses per unit length as a function of the incident solar radiation and the temperature difference between the HTF and the ambient air (Eduardo González-Mora et al., 2025), denoted as ΔT_{loss}:

$$\dot{q}'_{\text{loss}} = (8.3757 - 0.1194\Delta T_{\text{loss}} + 0.0014\Delta T_{\text{loss}}^2) + \frac{G_{\text{bn}}}{1000}(77.7499 + 0.0055\Delta T_{\text{loss}} + 0.00002\Delta T_{\text{loss}}^2) \qquad \text{(eq. 2)}$$

The mass flow rate in the solar field ($\dot{m}_{\text{SF}}$) is calculated using the thermal load specified in Table 2 as follows:

$$\dot{Q}_{\text{gain,HTF}} = SM\dot{Q}_{\text{load}} = \dot{m}_{\text{SF}} c_{\text{HTF}} \Delta T_{\text{HTF}} \qquad \text{(eq. 3)}$$

Equation (3) calculates the total mass flow rate of the HTF in the solar field ($\dot{m}_{\text{SF}}$) using the process load ($\dot{Q}_{\text{load}}$), the solar multiple (SM), the specific heat of the HTF (c_{HTF}), and the temperature difference of the HTF in the solar field (ΔT_{HTF}).

To guarantee an efficient heat transfer between the absorber tube of the PTC and the HTF, the total mass flow needs to be divided into parallel loops while maintaining a turbulent flow regime (Re$\sim 10^5$) with comparable flow velocity for each fluid. Dividing the mass flow rate into several loops determines the required number of parallel loops for the SHIP setup. Additionally, the loop lengths are established by iteratively evaluating the equations outlined in Eq. (1) until the HTF achieves the targeted temperature.

An SM greater than 1 implies the possibility of integrating thermal storage, which will allow supplying thermal energy even when the solar system is not in operation. This will considerably reduce the use of LPG. On days when the heat demand in the solar field is not 100% covered (days of low insolation), the LPG boiler will be able to supply thermal energy even when the solar system is not operating, as shown in Fig. 2. We determine the volume of the TES tank with the energy density of the HTF (E_{TES}):

$$V_{\mathrm{TES}}=\frac{SM\dot{Q}_{\mathrm{load}}t_{\mathrm{storage}}}{E_{\mathrm{TES}}} \quad \text{(eq. 4)}$$

3.2. Performance metrics

The energy and exergy efficiencies of the solar field are calculated by evaluating the ratio of fluid energy (or exergy) gain to the energy (or exergy) of solar radiation incident on the net mirror area. Eq, 5a defines energy efficiency, while Eq. 5b defines exergy efficiency. The exergy of solar radiation $\dot{Ex}_{\mathrm{DNI}}$) is calculated according to the endoreversible model developed by González-Mora et al. (2023). The overall energy and exergy efficiencies are determined by multiplying the efficiencies of the solar field (Eqs. 5a and 5b) with those for the refrigerator (as shown in Eqs. 6a and 6b).

$$\eta_{\mathrm{I,SF}}=\frac{\dot{Q}_{\mathrm{gain,HTF}}}{\dot{Q}_{\mathrm{inc}}}=\frac{\dot{m}_{\mathrm{HTF}}\Delta h_{\mathrm{HTF}}}{A_{\mathrm{SF}}DNI} \quad \text{(eq. 5a)}$$

$$\eta_{\mathrm{II,SF}}=\frac{\dot{Ex}_{\mathrm{gain,HTF}}}{\dot{Ex}_{\mathrm{inc}}}=\frac{\dot{m}_{\mathrm{HTF}}\Delta ex_{\mathrm{HTF}}}{A_{\mathrm{SF}}\dot{Ex}_{\mathrm{DNI}}} \quad \text{(eq. 5b)}$$

$$\eta_{\mathrm{I,tot}}=\beta\times\eta_{\mathrm{I,SF}} \quad \text{(eq. 6a)}$$

$$\eta_{\mathrm{II,tot}}=\eta_{\mathrm{II,ref}}\times\eta_{\mathrm{II,SF}} \quad \text{(eq. 6b)}$$

The pharmaceutical facility requires a thermal load of 292.2 kW to generate the cooling effect for its operations. This process currently relies on LPG as the primary fuel source. The facility consumes 782.9 kg of LPG per day, and with the cost of LPG in Mexico at 1 USD per kg, daily fuel expenses amount to 782.9 USD. Annually, this results in a total cost of 284185 USD. With the integration of the solar field, a significant reduction in LPG consumption can be expected, resulting in substantial economic savings. The daily LPG consumption is estimated using Eq. 7, while Eq. 8 allows estimating the daily cost.

$$\dot{m}_{\mathrm{fuel}}=\frac{\dot{Q}_{\mathrm{PTC}}-\dot{Q}_{\mathrm{load}}}{LHV} \quad \text{(eq. 7)}$$

$$\mathrm{Cost}_{\mathrm{fuel}}=\dot{m}_{\mathrm{fuel}}\times 1\ \mathrm{day}\times 1\,\frac{\mathrm{USD}}{\mathrm{kg}} \quad \text{(eq. 8)}$$

The reduction in greenhouse gas (GHG) emissions achieved by displacing LPG is calculated using its emission factor (EF) according to Eq. 9, along with the energy supplied by the LPG. The emission factors are obtained from the IPCC Guidelines for National Greenhouse Gas Inventories (IPCC, 2006), which standardize GHG emissions accounting for fossil fuels. For LPG, the emission factors are as follows: $EF_{\mathrm{CO_2}}$ =65600 kg/TJ , $EF_{\mathrm{CH_4}}$ =3 kg/TJ, and $EF_{\mathrm{N_2O}}$ =0.3 kg/TJ.

$$\Delta GHG_{\mathrm{fuel}}=\dot{m}_{\mathrm{fuel}}LHV_{\mathrm{fuel}}EF_{\mathrm{GHG,fuel}} \quad \text{(eq. 9)}$$

3.3. Simulation approach

The simulation approach for this study is anchored in design point conditions, which establish operating parameters optimized to maximize solar thermal system performance. Key variables such as solar irradiance, ambient temperature, and wind speed are defined at the design point, directly influencing the required concentrator field area. Following established convention, the design point is set for June 21 at solar noon—a period of peak solar field efficiency—to ensure accurate performance benchmarking under optimal conditions. These parameters, summarized in Table 3, include solar irradiance, ambient temperature, and HTF inlet/outlet temperatures, forming the basis for reliable system predictions.

Simulations evaluate the installation not only for the full design day but also across four representative days (solstices and equinoxes) and every day of the year. This multi-scale analysis captures daily and seasonal variations, enabling a comprehensive assessment of energy delivery, fuel consumption for refrigeration, solar fraction, operating hours, and system efficiencies (energy and exergy). Additionally, the capacity factor is calculated to quantify the system's utilization relative to its maximum potential. By integrating daily and annual simulations, the study ensures robust evaluation of the SHIP system's performance under diverse meteorological and operational scenarios.

Tab. 3: Design point conditions (Sengupta et al., 2018)

Parameter	Symbol	Value
Weather conditions		
Direct normal irradiance, (W/m^2)	DNI	691
Ambient temperature, (ºC)	T_0	23.7
Insolation hours, (bar)	t_{sun}	6.5
Location		
Latitude, (deg)	Φ_{loc}	19.29
Longitude, (deg)	L_{loc}	-99.65
Altitude, (m)	A_{loc}	2700
Solar field HTF conditions		
Inlet temperature, (ºC)	$T_{\mathrm{HTF,in}}$	185
Outlet temperature, (ºC)	$T_{\mathrm{HTF,out}}$	210

4. Results

4.1. Solar field sizing and configuration

The thermodynamic model outlined in Section 3 determines the solar field size for both system configurations (with and without TES), with the design day fixed on June 21 at solar noon. For the TES-integrated system, a solar multiple (SM) of 1.5 requires a solar field area of 1350 m^2 and a TES volume of 28.16 m^3, providing 2.5 hours of storage. Energy and exergy efficiencies are 0.645 and 0.11, respectively. The non-TES system, with an SM of 1, uses a 900 m^2 solar field while maintaining identical efficiencies. In both cases, the available 2000 m^2 roof area comfortably accommodates the solar field.

The following subsections will analyze the operational dynamics of these configurations in detail, including annual performance variations, fuel consumption patterns, and system utilization metrics under real-world conditions.

4.2. Design and representative days performance

The analysis of the four representative days (equinoxes and solstices) underscores significant operational contrasts between the SHIP installations with and without thermal energy storage (TES). Figures 3, depicting hourly thermal power (3a, 3b) and efficiencies (3c, 3d), reveal distinct performance patterns. For the TES-equipped system, March 21 (equinox) yielded a delivered energy surplus (3,996.65 kWh versus required 3,360.30 kWh), producing negative fuel consumption (-47.35 kg) and a solar fraction of 118.94%, highlighting TES's capacity to offset auxiliary fuel reliance during favorable solar conditions. By contrast, the design day (June 21) saw a solar fraction of 62.68% with 93.34 kg of fuel required, reflecting increased thermal demand and reduced solar contribution in peak summer. Seasonal declines further reduced performance on September 21 (solar fraction: 39.32%, fuel: 151.76 kg) and December 21 (solar fraction: 62.34%, fuel: 94.19 kg). Energy and exergy efficiencies remained consistent (0.18–0.24 and 0.06–0.09, respectively), while capacity factors varied between 39.13% and 52.17%.

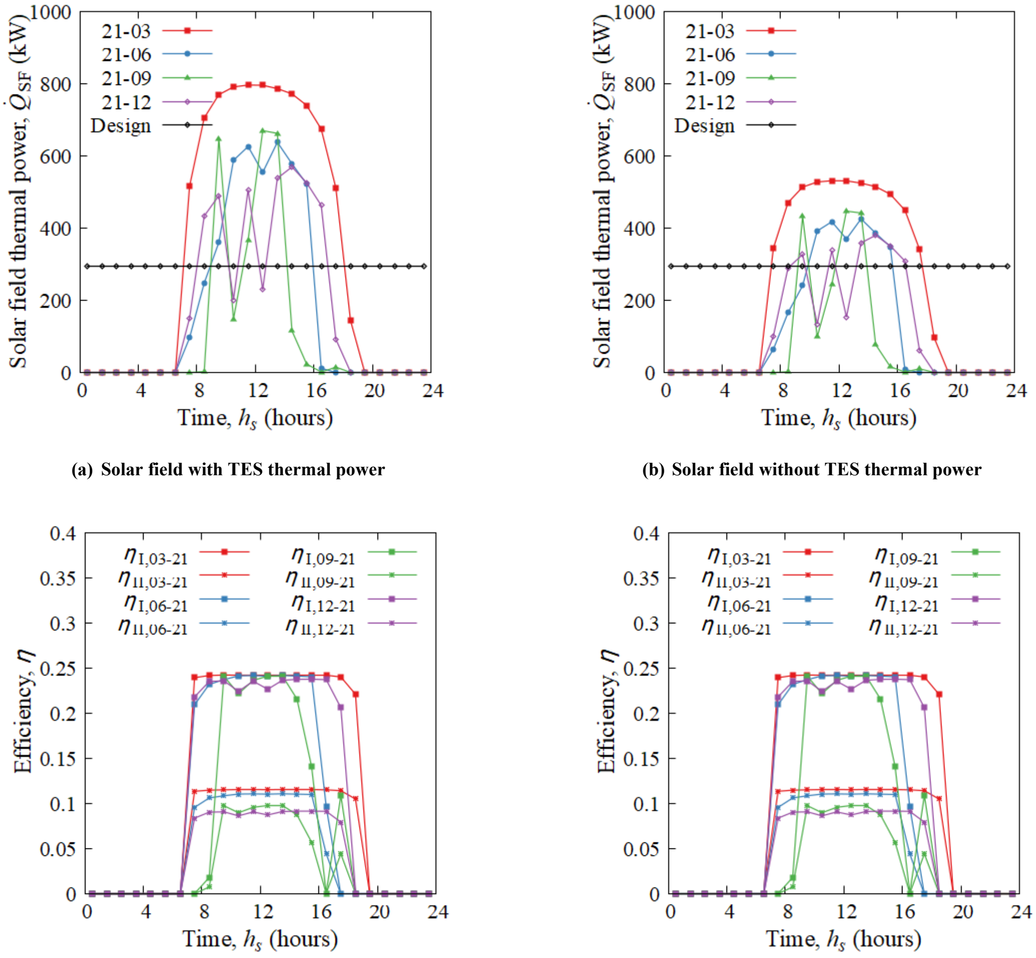

(a) Solar field with TES thermal power

(b) Solar field without TES thermal power

(c) Efficiencies for SHIP with TES

(d) Efficiencies for SHIP without TES

Fig. 3: Representative days results. SHIP with TES.

The non-TES system exhibited markedly higher fuel dependency across all days. On March 21, its solar fraction dropped to 79.29% (fuel: 51.80 kg), with no energy surplus. June and December 21 saw fuel use surge to 145.59 kg and 146.16 kg (solar fractions: 41.79% and 41.56%), while September 21 recorded the poorest performance (solar fraction: 26.21%, fuel: 184.54 kg). Though energy and exergy efficiencies aligned closely with the TES system (0.18–0.24 and 0.04–0.08), the absence of storage amplified fuel reliance during low-irradiance periods.

Key differences emerge in fuel savings and solar utilization. TES enabled fuel reduction or elimination on March 21 (-47.35 kg versus +51.80 kg without TES) and sustained higher solar fractions year-round, particularly in shoulder seasons (March/December: >60% versus ≤41.79% without TES). Efficiency parity between systems suggests TES primarily enhances reliability rather than thermodynamic performance, as evidenced by smoother thermal power profiles in Figures 3a–4b. These dynamics illustrate TES's role in mitigating solar intermittency, though its benefits diminish during peak demand periods. The following subsection expands this analysis to annual performance, contextualizing these findings within broader operational trends.

4.3. Annual performance

The annual performance analysis, illustrated in Fig. 4 (thermal power), highlights critical distinctions between the SHIP systems with and without TES. The TES-integrated system delivered 780,328.51 kWh annually, covering 60.98% of the total energy demand (1,279,689.90 kWh), while the non-TES system supplied 520,219.59 kWh, achieving a solar fraction of 40.65%. This disparity underscores TES's role in mitigating solar intermittency, as evidenced by the 37167.30 kg of auxiliary fuel required with TES compared to 56525.48 kg without—a 34% reduction in fuel dependency.

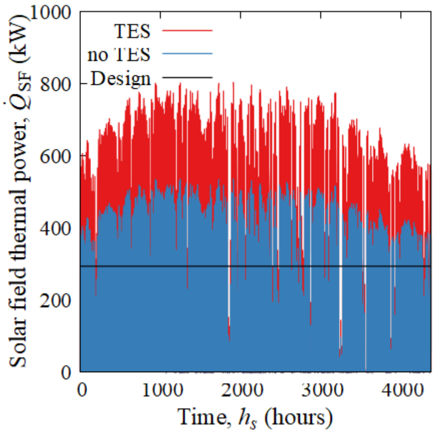

Fig. 4: SHIP performance over the year.

Hourly thermal power profiles reveal that TES stabilizes energy delivery, buffering transient solar losses and extending productive operation during low-irradiance intervals. This smoothing effect is particularly evident in reduced fuel consumption peaks, aligning with the annual fuel savings. Despite identical operating hours (1,887.50 h) and capacity factors (43.10%), the TES system's superior solar utilization demonstrates its operational resilience. Energy efficiencies for both systems matched (0.22), but the non-TES configuration exhibited a marginally higher exergy efficiency (0.08 versus 0.06), likely due to avoided thermal losses from storage and smaller solar field.

The divergence in solar fractions (60.98% vs. 40.65%) emphasizes TES's capacity to enhance annual energy harvest, though thermodynamic efficiencies remain constrained by system design and ambient conditions. These findings affirm that TES significantly bolsters fuel savings and reliability without fundamentally altering energy conversion efficiency. The results underscore the trade-off between enhanced solar utilization and incremental exergy losses, positioning TES as a pragmatic solution for industrial applications prioritizing fuel reduction over marginal efficiency gains.

4.4. Technical-economic and environmental feasibility

The integration of a solar field with TES demonstrates significant technical and operational advantages, as evidenced by the annual solar fraction of 60.98% (with TES) versus 40.65% (without TES). This highlights TES's role in stabilizing energy supply, reducing reliance on auxiliary fuel by 34% compared to the non-TES system. Both configurations share identical operating hours (1,887.50 h) and capacity factors (43.10%), confirming comparable baseline operability, but TES enhances reliability by mitigating solar intermittency through energy buffering.

Economically, the SHIP system with TES reduces annual fuel costs to $37167.30—an 87% savings compared to the non-solar baseline ($285750). The non-TES system, while still cost-effective relative to the baseline, incurs higher fuel expenses ($56525.48), underscoring TES's financial benefit. Environmentally, TES achieves an 86.99% reduction in CO2 emissions (117939 kg vs. 906745 kg baseline), outperforming the non-TES system (70.33% reduction, 179367 kg CO2). Similar trends apply to CH4 and N2O emissions, with TES lowering methane and nitrous oxide outputs by 87% and 86%, respectively, compared to 80% and 80% without TES.

These results underscore TES's dual advantage: it not only enhances technical feasibility through consistent energy delivery but also delivers superior economic and environmental returns. While both systems reduce emissions and costs substantially relative to fossil-only operation, TES's ability to store surplus solar energy translates into markedly lower annual fuel consumption and pollutant release. This positions TES as a critical enabler for industrial decarbonization, balancing operational reliability with sustainability goals, albeit at potential upfront infrastructure costs not quantified here.

5. Conclusions

This study set out to evaluate the technical performance and LPG-saving potential of a parabolic trough collector (PTC)–driven absorption cooling system in a pharmaceutical facility in Toluca, México, comparing configurations with and without thermal energy storage (TES). We applied an in-house validated thermohydraulic model to size the solar field, simulate design-day and annual operation, and compute energy, exergy, and fuel-consumption metrics under realistic irradiance and load profiles.

We demonstrated that a 900 m² PTC field without TES and a 1350 m² field with 28.16 m³ of TES meet the 118.2 kW cooling demand at −10 °C, achieving design-day solar COPs of 0.2407 and 0.2219, respectively. The study reveals daily LPG reductions of up to 500 kg (≈USD 300) and annual solar fractions of 40.65 % (no TES) and 60.98 % (with TES), corresponding to a 34 % decrease in auxiliary fuel use when TES is in place.

We encountered limitations related to industry confidentiality, which prevented detailed cost-and-maintenance analyses, and modeling assumptions that may understate thermal losses within the storage tank. These constraints may affect the precision of projected economic benefits and exergy-efficiency figures.

By quantifying both energy and exergy performance in a pharmaceutical context—an area scarcely addressed in prior Mexican studies—this work advances the field beyond conventional solar-cooling applications in food processing and mining. The results align with established findings on TES's ability to mitigate intermittency while offering new insights into rooftop PTC deployment under constrained area conditions. Future research should integrate real-world financial data to refine the cost–benefit analysis, validate system performance through pilot-scale implementations, and optimize TES charge/discharge control strategies.

6. Acknowledgments

This work was partially funded by COMECyT grant CAT2024-0112 (AESCo project), which supported Eduardo González-Mora through the *Programa Investigadoras e Investigadores*.

7. References

Cabeza, L.F., 2014. Advances in Thermal Energy Storage Systems : Methods and Applications, 1st ed. Elsevier. https://doi.org/2015

Cabrera, F.J., Fernández-García, A., Silva, R.M.P., Pérez-García, M., 2013. Use of parabolic trough solar collectors for solar refrigeration and air-conditioning applications. Renewable and Sustainable Energy Reviews 20, 103–118. https://doi.org/10.1016/j.rser.2012.11.081

Eduardo González-Mora, Ma. Dolores Durán-García, Álvaro Lentz-HErrera, 2025. Expected year performance and economic evaluation for the integration of a small-scale ptc in a tequila company, in: 38th International Conference on Efficiency, Cost, Optimization, Simulation and Environmental Impact of Energy Systems– ECOS 2025. Paris.

Esfanjani, P., Jahangiri, S., Heidarian, A., Valipour, M.S., Rashidi, S., 2022. A review on solar-powered cooling systems coupled with parabolic dish collector and linear Fresnel reflector. Environmental Science and Pollution Research 29, 42616–42646. https://doi.org/10.1007/s11356-022-19993-3

González-Mora, E., Durán-García, M.D., 2024. Alternative Approach for Thermo-Hydraulic Modeling of Direct Steam Generation in Parabolic Trough Solar Collectors. J Therm Sci Eng Appl 16, 1–12. https://doi.org/10.1115/1.4064819

González-Mora, E., Poudel, R., Durán-García, M.D., 2023. A practical upper-bound efficiency model for solar power plants. Journal of Non-Equilibrium Thermodynamics. https://doi.org/10.1515/jnet-2022-0080

IEA, 2018. The Future of Cooling. Paris.

Inventive Power, 2013. POWER TROUGH 250 [WWW Document]. URL https://inventivepower.com.mx/solucion-en-energia-solar/power-trough-250/ (accessed 1.3.24).

IPCC, 2006. Stationary Combustion, 2006 IPCC Guidelines for National Greenhouse Gas Inventories. Hayama, Japan.

Karellas, S., Roumpedakis, T.C., Tzouganatos, N., Braimakis, K., 2018. Solar cooling technologies, 1st ed. CRC Press.

Mahmood, Y., 2020. A Review of a Mechanical Vapour Compression Refrigeration System: Environment and Performance Challenge, in: Proceedings of the Proceedings of the 1st International Multi-Disciplinary Conference Theme: Sustainable Development and Smart Planning, IMDC-SDSP 2020, Cyperspace, 28-30 June 2020. EAI. https://doi.org/10.4108/eai.28-6-2020.2298158

Moya, E.Z., 2021. Parabolic-trough concentrating solar power systems, in: Concentrating Solar Power Technology. Elsevier, pp. 219–266. https://doi.org/10.1016/B978-0-12-819970-1.00009-8

Ouali, M., Abbad, B., Bouabdallah, A., 2014. Conception and experimental study of a solar vaccine refrigerator powered by a hybrid system, in: Refrigeration Science and Technology. pp. 211–218.

Permana, I., Wang, F., 2024. Performance improvement of a biotechnology vaccine cleanroom for contamination control. Journal of Building Engineering 82, 108248. https://doi.org/10.1016/j.jobe.2023.108248

REN21, 2024. Renewables 2024 Global Status Report Collection, Renewables in Energy Demand. Paris.

Sengupta, M., Xie, Y., Lopez, A., Habte, A., Maclaurin, G., Shelby, J., 2018. The National Solar Radiation Data Base (NSRDB). Renewable and Sustainable Energy Reviews 89, 51–60. https://doi.org/10.1016/j.rser.2018.03.003